Eur. Phys. J. E (2015) **38**: 47
DOI 10.1140/epje/i2015-15047-x

THE EUROPEAN PHYSICAL JOURNAL E

Regular Article

Transient dynamics of a 2D granular pile

Patrick Mutabaruka[1,a], Krishna Kumar[3], Kenichi Soga[3], Farhang Radjai[1,4], and Jean-Yves Delenne[2]

[1] LMGC, UMR 5508 University Montpellier 2 – CNRS, F-34095 Montpellier cedex 5, France
[2] IATE, UMR1208 INRA – University Montpellier 2 – Cirad – Montpellier Sup Agro, F-34060 Montpellier cedex 1, France
[3] Cambridge University, Engineering Department, Cambridge CB2 1PZ, UK
[4] MultiScale Material Science for Energy and Environment, UMI 3466 CNRS-MIT, CEE, Massachusetts Institute of Technology, 77 Massachusetts Avenue, Cambridge 02139, USA

Received 20 January 2015 and Received in final form 9 March 2015
Published online: 26 May 2015 –

Abstract. We investigate by means of Contact Dynamics simulations the transient dynamics of a 2D granular pile set into motion by applying shear velocity during a short time interval to all particles. The spreading dynamics is directly controlled by the input energy whereas in recent studies of column collapse the dynamics scales with the initial potential energy of the column. As in column collapse, we observe a power-law dependence of the runout distance with respect to the input energy with nontrivial exponents. This suggests that the power-law behavior is a generic feature of granular dynamics, and the values of the exponents reflect the distribution of kinetic energy inside the material. We observe two regimes with different values of the exponents: the low-energy regime reflects the destabilization of the pile by the impact with a runout time independent of the input energy whereas the high-energy regime is governed by the input energy. We show that the evolution of the pile in the high-energy regime can be described by a characteristic decay time and the available energy after the pile is destabilized.

1 Introduction

Most contemporary research on granular materials deals with the steady-state flow [1–4]. Transients and inhomogeneous boundary conditions are much less amenable to observation and analysis, and have thus been less well studied despite their primary importance in engineering practice [5–7]. In the geological context, for example, transient movements of large granular slopes and heaps are of special interest with regard to their destructive force and the transformations that they may produce in the landscape [8–10]. Such movements may be induced by the action of various forces and energy sources such as sudden rock fall, tsunamis or earthquakes [11,12]. In all cases, an initially static pile of grains is first disturbed by external forces, it then undergoes an abrupt accelerated motion and spreads over long distances before relaxing to a new equilibrium state when the whole kinetic energy acquired during destabilization is dissipated by friction and inelastic collisions.

Such transient flows have been studied by laboratory experiments and simulations in different geometries such as tilted piles for slope failure and surface avalanches [13–16] or by considering vertical columns of grains collapsing and spreading under their own weight [17–21]. The dynamics is often found to be nontrivial in the sense that the final configurations after the whole kinetic energy is dissipated can not readily be predicted by means of simple arguments based on the Mohr-Coulomb nature of the material or dimensional analysis. For example, in the case of collapsing columns the runout distance is found to obey a power-law dependence with the initial aspect ratio of the column [18,20,21]. In a similar vein, the avalanche volume is found to be controlled by two angles rather than a single Coulomb angle (corresponding to the internal friction angle of the material) [22,23,19]. Nontrivial features of this kind are often also correctly reproduced by simulations using discrete element method (DEM) and analyzed at the grain scale [22,24–29]. This indicates that the origins of such complex behaviors are due to collective behaviors and long-range velocity correlations [30] or possibly inertial effects, which may play a crucial role during transient flows.

An interesting issue is how generic are such power-laws and whether trivial exponents may arise in configurations which are simpler than collapsing columns. In this paper, we analyze such a configuration: a granular pile initially at rest subjected to a horizontal impact. In contrast to the column geometry, the driving force in this configuration is not the initial potential energy since the pile is in static equilibrium at its angle of repose. Instead, the kinetic energy is directly supplied to the whole pile, which is set

[a] e-mail: patrick.mutabaruka@univ-montp2.fr

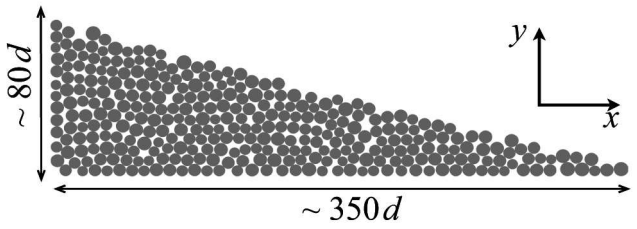

Fig. 1. Initial geometry and dimensions of the pile.

into motion and flows over a finite distance. This "quake" applied to the pile may represent a real scenario such as a seismic slope failure, but here we are interested in the transient dynamics of a simple configuration. The initial kinetic energy fed by the quake into the pile can be compared to the kinetic energy released during the collapse of a granular column. The runout of a collapsing granular column as a function of the kinetic energy available at the end of free fall has been recently investigated [28]. An interesting finding was that the effect of a fluid on the runout distance can be expressed as a function of this kinetic energy rather than the initial aspect ratio of the column.

For this investigation, we rely on Contact Dynamics (CD) simulations, in which the particles are modeled as infinitely rigid bodies, governed by Newton's equation of motion, that interact through frictional contacts [31–33]. We consider in detail the evolution of the pile, its runout distance and lifetime as a function of the input energy. Furthermore, we consider the time evolution of the kinetic energy and its scaling with the input energy. We introduce a characteristic time that reveals two regimes and two successive phases during evolution. We also investigate the effect of friction and restitution coefficients on the runout.

We first present in sect. 2 the numerical methods and procedures employed in the simulations. Then, we consider the evolution of the shape of the granular pile in sect. 3, in particular the runout distance and its dependence on the input energy. In sect. 4, we study the evolution of the kinetic energy and the scaling of runout by introducing a characteristic time. Then, in sect. 5, we focus on the effect of local dissipation parameters.

2 Numerical procedures

The numerical samples are composed of $\sim$ 13000 disks with a uniform distribution of diameters by volume fractions in the range $[d_{\min}, d_{\max}]$ with $d_{\max} = 1.5d_{\min}$. The mean particle diameter and mass are $d \simeq 0.0025\,\mathrm{m}$ and $m \simeq 0.0123\,\mathrm{kg}$, respectively. The particles are first poured uniformly into a rectangular box of given width and then the right-hand side wall is shifted further to the right to allow the particles to spread. A granular talus is obtained when all particles come to rest; see fig. 1. This procedure leads to a mean packing fraction $\simeq 0.83$. Three different values of the friction coefficient $\mu_s = \{0.1, 0.4, 0.7\}$ and normal and tangential coefficients of restitution $e_n = e_t = \{0, 0.4, 0.8\}$ are used and for each combination of these parameters 10 independent initial configurations were considered.

The initial static pile is set into motion by applying a constant vertical velocity gradient to the particles:

$$v_{0x}(y) = k(y_{\max} - y), \tag{1}$$

with $k > 0$. In other words, at $t = 0$, the particles are assigned a velocity v_{0x} in the x-direction with v_{0x} depending linearly on the y-position. No energy is supplied to the vertical and rotational degrees of freedom of the particles. Such a configuration mimics the energy transfer mechanism of a horizontal quake along the bottom of the pile. We are interested in the evolution of the geometry of the pile and its total kinetic energy as a function of the initial input energy E_0 per particle. The runout distance R_f is the distance of the rightmost particle, which is still in contact with the main mass, from the left wall when the pile comes to rest. It will be normalized by the initial length R_0 of the pile, as in the experiments of collapsing columns. The total runout duration t_f is the time that the pile takes to reach its final runout distance R_f.

DEM simulations are performed using the CD method. A detailed description of this method can be found in [31–34]. This method is based on implicit time integration of the equations of motion and a nonsmooth formulation of mutual exclusion and dry friction between particles. The CD method requires no elastic repulsive potential and no smoothing of the Coulomb friction law for the determination of forces. For this reason, the simulations can be performed with large time steps compared to molecular dynamics simulations. The unknown variables are particle velocities and contact forces, which are calculated at each time step by taking into account the conservation of momenta and the constraints due to mutual exclusion between particles and the Coulomb friction. We use an iterative research algorithm based on a nonlinear Gauss-Seidel scheme. The only contact parameters within the CD method are the friction coefficient μ_s, the normal restitution coefficient e_n and the tangential restitution coefficient e_t between particles. We will investigate the effect of these parameters on the evolution of kinetic energy and the profile of the pile.

The natural units of our system are the mean particle diameter d, mean particle mass m and gravity g. For this reason, in the following we normalize the lengths by d, the times by $(d/g)^{1/2}$, the velocities by $(gd)^{1/2}$ and the energies by mgd. Note that two different representations of a 2D system are possible. In the first representation, the 2D volume of a particle is simply its area $\pi * d^2/4$ and the density is expressed as mass per unit area. We used a density of $2500\,\mathrm{kg/m^2}$. In the second representation, the particles are assumed to be cylinders of unit length. If this interpretation is used, the volume of a particle is again given by $\pi * d^2/4$ and the density is $2500\,\mathrm{kg/m^3}$. In this case, the length/diameter radio is $1/d = 400$. This corresponds to a long cylinder and not a 2D object. However, if 2D simulations are accepted as a means to investigate the collective behaviour of granular materials, then both interpretations

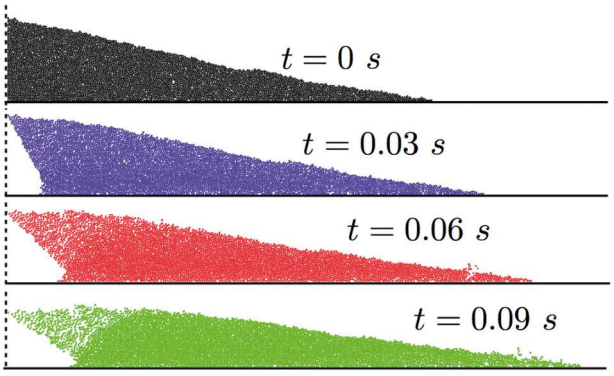

Fig. 2. Snapshots of the evolution of the pile profile for $E_0 = 61\ mgd$.

are basically equivalent. This is because a cylinder whose motion is restricted to take place in a plane and perpendicular to its axis, is no more than a simple disk. In other words, its third dimension is not an observable quantity.

Video samples of the simulations analyzed in this paper can be found by following the link `http://www.cgp-gateway.org/ref018`.

3 Evolution of pile geometry and runout

In this section, we consider the spreading process following the initial input energy in the pile. Figure 2 shows several snapshots of the pile for an initial input energy $E_0 = 61$ (in dimensionless units). The pile is sheared from the bottom to the top, thus leaving a cavity in the vicinity of the left wall. The cavity is partially filled while the pile continues to spread to the right.

Figure 3 shows the normalized runout distance $(R_f - R_0)/R_0$ and total runout time t_f as a function of the input energy E_0. We observe two regimes both characterized by a power-law runout distance and time as a function of E_0. In the first regime, corresponding to the range of low input energies $E_0 < 40\ mgd$, the runout distance varies as $R_f \propto (E_0)^{\alpha}$ with $\alpha \simeq 0.61 \pm 0.04$ over one decade while the duration keeps a constant value $t_f \simeq 60\ (d/g)^{0.5}$ irrespective of the value of E_0. The error on the value of the exponent represents the confidence interval of linear fits on the logarithmic scale. An average runout speed can be defined from the ratio $v_s = (R_f - R_0)/t_f$. According to the data, we have $v_s \propto (E_0)^{0.61\pm0.04}$. Since the initial average velocity varies as $v_0 \propto (E_0)^{0.5}$, this difference between the values of the exponents suggests that the mobilized mass during runout declines when the input energy is increased. As we shall see below, the constant runout time reflects also the collapse of the particles into the cavity left behind the pile.

In the second regime, corresponding to the range of high input energies ($E_0 > 40\ mgd$) the runout distance varies as $R_f \propto (E_0)^{\alpha'}$ over one decade with $\alpha' \simeq 0.77 \pm 0.03$ while the duration increases as $t_f \propto (E_0)^{\beta'}$ with $\beta' \simeq 0.21 \pm 0.04$. Hence, in this regime the average runout speed

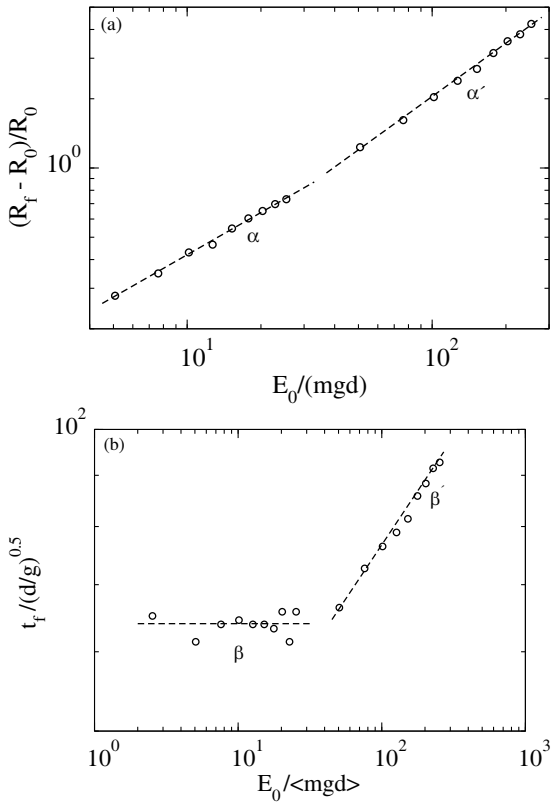

Fig. 3. Runout distance (a) and its duration (b) for different initial values of kinetic energy per particle. The dashed lines represent power-law fits to the data points in two different regimes with the their exponents.

varies as $v_s \propto (E_0)^{0.56\pm0.07}$. This exponent is close to the value 0.5 in $v_0 \propto (E_0)^{0.5}$, and hence, within the confidence interval of the exponents, in the second regime we may assume $\beta' \simeq \alpha' - 0.5$ and $v_s \propto v_0$.

It is worth noting that a similar power-law dependence of the runout distance and time were found in the case of collapsing columns of grains with respect to the initial aspect ratio [28]. In the column geometry, the particles spread away owing to the kinetic energy acquired during gravitational collapse of the column. Topin *et al.* [28]. found that the runout distance varies as a power-law of the available peak kinetic energy at the end of the free-fall stage with an exponent $\simeq 0.5$. This value is below those obtained here for both regimes. This is, however, physically plausible since the distribution of particle kinetic energies at the end of the collapse is more chaotic than in our simulations where the energy is supplied from the very beginning in a well-defined shear mode. As pointed out by [25], the distribution of kinetic energies is an essential factor for the runout distance.

4 Decay of kinetic energy

The nontrivial evolution of the pile geometry in two regimes suggests that the energy supplied to the pile is

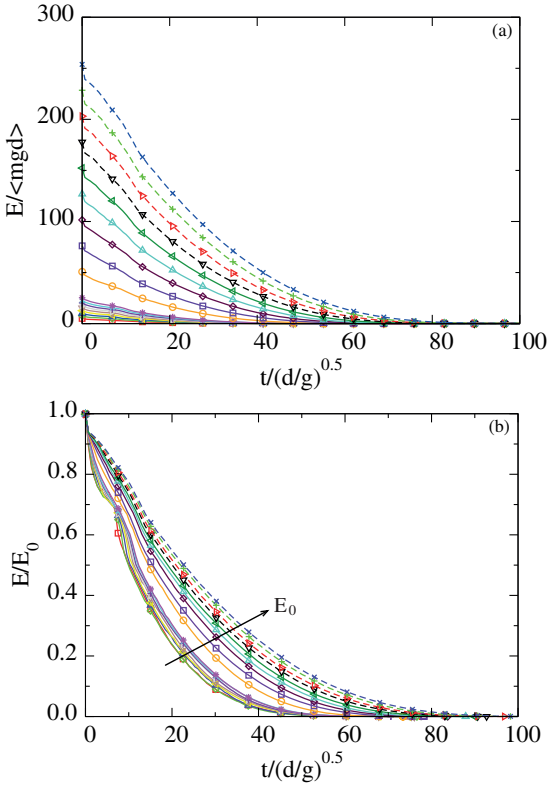

Fig. 4. Evolution of kinetic energy per particle with time normalised by mgd (a), and by the initial kinetic energy E_0 per particle (b) for different values of the initial kinetic energy per particle.

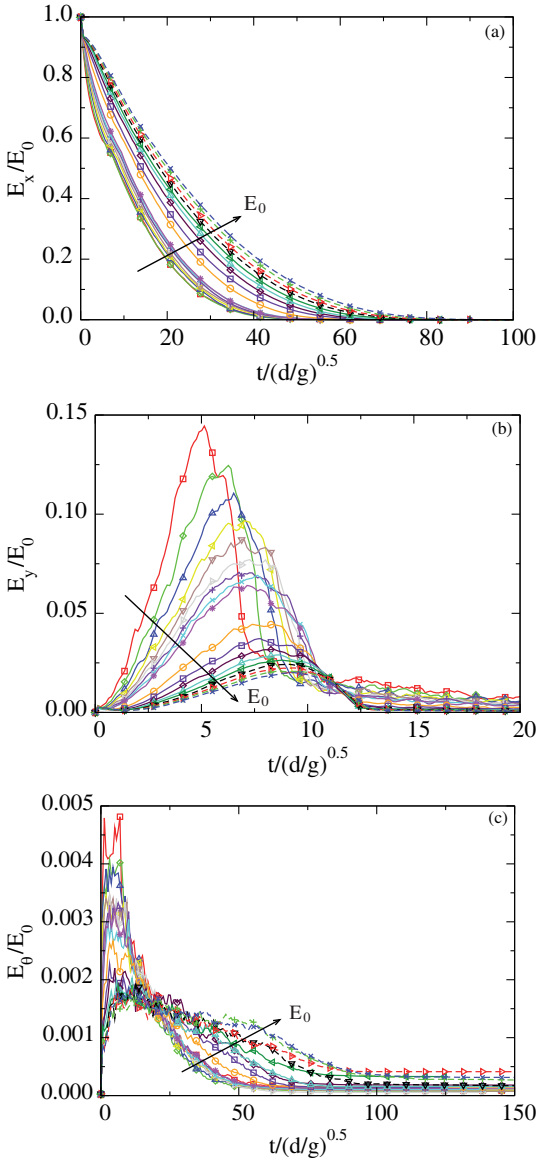

Fig. 5. Evolution of kinetic energy with time. (a) "horizontal" direction; (b) "vertical" direction and (c) "rotational" kinetic energies as a function of time.

not simply dissipated by shear and friction with the bottom plane. We also need to split the kinetic energy into its different components (x, y and rotation) of the velocity field. The input energy is in the x component, but due to both the creation of a cavity next to the left wall and the rolling of the particles down the free surface of the pile and between particles, a fraction of the energy is first transferred to the y component of the velocity field and dissipated during the transient phase. In this section, we analyze these features in order to arrive at a picture that is consistent with the evolution of the pile shape.

The decay of the total kinetic energy E is displayed in fig. 4(a) for different values of the input energy E_0. We observe an initial fast decay of E followed by a regular fall-off until the end of the runout. This regular fall-off occurs clearly with two different functional forms, thus unveiling two stages in the evolution of the pile. fig. 4(b) shows the same plots normalized by E_0. We see that all plots corresponding to the first regime (low energies) collapse nearly on a single time evolution. This is consistent with the fact that, as previously shown, in this regime the runout time t_f is independent of the input energy. In contrast, the plots for the second regime (high energies) collapse only at the beginning of runout, *i.e.* for $t < t_1 \simeq 7.5\ (d/g)^{0.5}$, where t_1 is the duration of the first stage.

Figure 5 displays the evolution of kinetic energy in the translational (E_x and E_y) and rotational (E_θ) degrees of freedom of the particles. E_x decays similar to the total energy, but E_y and E_θ increase and peak before decaying rapidly to a negligibly small level. The transient phase is best observed for E_y, which has significant values only for $t < t_1$. This energy represents the fraction of kinetic energy transferred to the y component of the velocity field due to the destabilization of the pile and collapse of particles in the cavity behind the pile. We note that lower the E_0, the higher the peak value of E_y/E_0. This means that, at low values of the input energy a larger fraction of input energy E_0 is consumed in the destabilization process whereas at a high level of input energy most of it is dissipated in the spreading phase. For this reason, the total duration t_1 of this destabilization transient is nearly the same in both regimes and its value is controlled by the

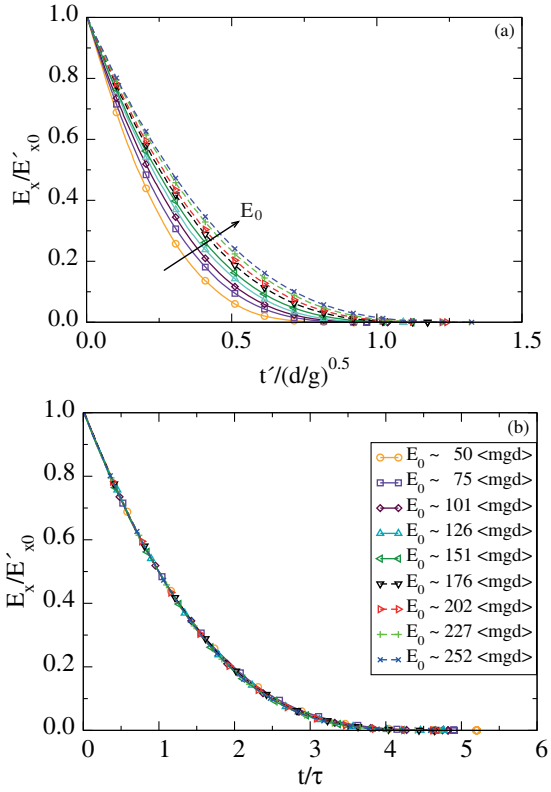

Fig. 6. Evolution of kinetic energy in the x component of the velocity field normalized by the available kinetic energy at the end of the destabilization transient as a function of time elapsed since the same instant (a) and as a function of normalized time (b).

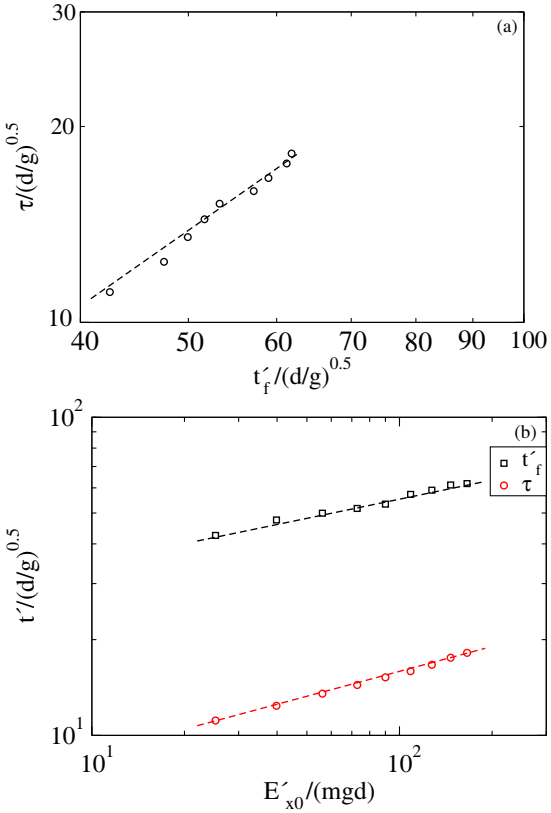

Fig. 7. Linear relationship between decay time and runout time following destabilization transient (a), and power-law evolution of t'_f and τ as a function of kinetic energy E_{x0} in the x component (b).

gravity rather than the input energy. The height of the pile being of the order of 80 d, the total free-fall time for a particle located at this height is $\simeq 12\ (d/g)^{0.5}$, which is of the same order as the duration t_1 of the first stage. As to the rotational energy, its contribution both to the destabilization transient and subsequent spreading is negligible.

To analyze the second phase in the second regime, we now consider only the kinetic energy E'_{x0} available at the end of the destabilization phase. This energy is responsible for most of the runout and hence it is expected to control the runout distance and time. Figure 6(a) shows the evolution of E_x normalized by E'_{x0} as a function of time. The plots show the same aspect but they have different decay times. A decay time τ can be defined as the time required for E_x to decrease by a factor 1/2. Figure 6(b) shows the same data in which the time t' elapsed since t_1 is normalized by τ. Interestingly, now all the data nicely collapse on the same curve. We checked that this curve can not be fitted by simple functional forms such as variants of exponential decay. This means that the spreading of the pile is not a self-similar process. This observation is in agreement with the fact that the energy fades away in a finite time t'_f.

The scaling of the data with decay time τ also suggests that the runout time t'_f since the beginning of the second phase might be a simple function of τ. Figure 7 shows both t'_f and τ as a function of E'_{x0}, where we observe a power-law for both times over nearly one decade. The runout time $t'_f \propto (E'_{x0})^{\beta'}$ has the same exponent $\beta' \simeq 0.21 \pm 0.03$ as t_f as a function of E_0 (see fig. 3). For the decay time we have $\tau \propto (E'_{x0})^{\beta''}$ with $\beta'' \simeq 0.28 \pm 0.03$. The relation between the two times can thus be expressed as

$$t'_f = k\,\tau\,(E'_{x0})^{\beta''-\beta'}, \qquad (2)$$

where $k \simeq 5 \pm 0.4$ and $\beta'' - \beta' \simeq -0.05 \pm 0.06$. This difference in value is small enough to be neglected within the confidence interval of our data. It is therefore plausible to assume that the runout time is a multiple of the decay time and the spreading process is controlled by a single time. We however note that a weak dependence on the energy E'_{x0} is consistent with the fact that the whole available energy at the beginning of the second phase is not dissipated in the spreading process (calculated from the position of the tip of the pile) since the pile keeps deforming by the movements of the particles at the free surface even when the tip comes to rest. This can explain the small difference between the two measured exponents.

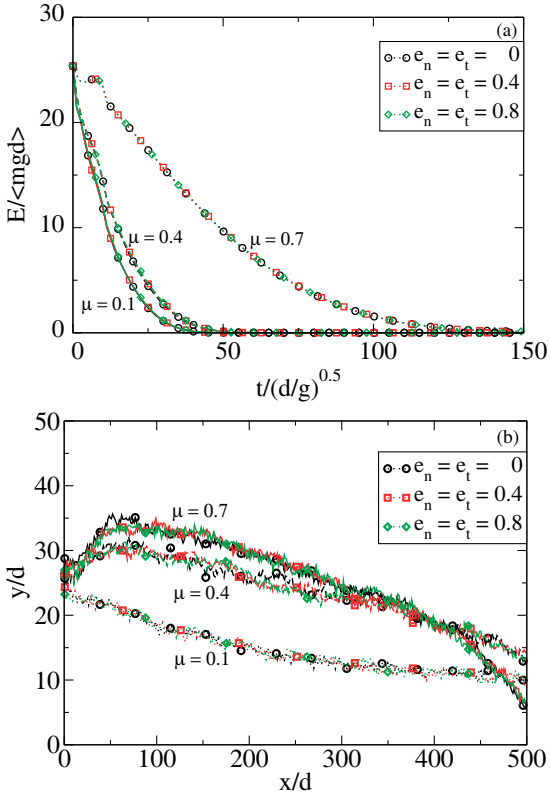

Fig. 8. Kinetic energy (a) and pile profile (b) for three values of the friction coefficient μ_s and for different values of the restitution coefficient $e_n = e_t$.

5 Effect of local parameters

The runout distance, runout duration and the dissipation of kinetic energy are controlled by the input energy and the collective dynamics of the whole pile, as analyzed in the previous sections. But they are expected to depend also on the friction and restitution coefficients, μ_s, e_n and e_t at the contact scale. We performed a series of simulations with different values of μ_s and $e_n = e_t$ for $E_0 = 25$ mgd. The results are shown in fig. 8 for the profiles of the pile and evolution of the kinetic energy with time. We see no difference in the dynamics for different values of $e_n = e_t$. This is a consequence of the highly dissipative nature of the material such that, even at large input energies, the pile remains in a dense state so that multiple collisions inside the pile occur at small time scales compared to the deformation time. When the restitution coefficients are increased, more collisions occur during a longer time interval but the overall energy dissipation rate by collisions remains the same. This effect is a seminal example of collective effects which erase the influence of local parameters at the macroscopic scale.

In contrast to the restitution coefficients, the effect of the friction coefficient is quite important for the runout, as observed in fig. 8 for both the energy decay and geometrical profile of the pile. Both the runout distance and decay time decrease as the friction coefficient is increased. This effect is much more pronounced at low values of the friction coefficient. The runout time is reduced by a factor 4 as μ_s is increased from 0.1 to 0.4 while the runout times and profiles do not change much for $\mu_s = 0.7$. This level-off effect was evidenced in a systematic way in simple shear tests, and it was attributed to the self-organization of the structure such that the dilation of the granular material and rolling of the particles change in response to the increase of the friction coefficient to keep the same level of dissipation rate [35].

6 Conclusion

In this paper, we investigated the runout behavior of a pile set into motion by applying shear velocity during a short time interval to an initially static granular pile. The choice of this geometry was motivated by our goal to focus on the effect of input energy on the consecutive dynamics of a granular material. For the range of input energies investigated in this pushing test by means of contact dynamics simulations, we observed a power-law dependence of the runout distance and time with nontrivial exponents. In our view, this is a central message of this work as it suggests that the power-law behavior is a generic feature of granular dynamics. In other words, the values of the exponents are not simple functions of the geometry or local material parameters. Such power-laws indicate that the distribution of kinetic energies inside the material is important for the dynamics. In a way, the supplied energy at the scale of the pile is not simply dissipated at the bottom plane or homogeneously inside the pile. As suggested by the turbulence-like scaling of nonaffine velocity fields previously evidenced by simulations, the energy is dissipated at different scales down to the particle scale [30]. This feature needs further analysis in the sandpile geometry, but it is likely to provide a plausible physical picture underlying power-laws in the dynamics of granular materials.

We also evidenced two regimes with different values of the exponents: a low-energy regime and a high-energy regime. The first regime reflects mainly the destabilization of the pile by the initial impulse with a runout time independent of the input energy whereas the second regime is governed by the spreading dynamics induced by the higher value of the input energy. We showed that the evolution of the pile in this high-energy regime can be described by a characteristic decay time and the energy available at the end of the first stage where the pile is destabilized by the impulse.

This work may be pursued by analyzing the scaling of velocity fields and also by experimental realization of a similar setup with increasing value of the input energy as well as 3D simulations. Although numerical simulations are generally reliable with often realistic results in studies of steady flows, we believe that the transients are more sensitive situations than steady states and the experiments are necessary for checking full validity of simulation results. Provided a convenient method is used for supplying kinetic energy homogeneously into a pile, our configuration is also interesting for the investigation of the behavior of a pile immersed in a viscous fluid. Finally,

it seems to us also interesting to consider different modes of energy injection. For example, the pile can be set into motion by sudden horizontal motion of the base or equal impulse applied to all particles. We investigated some of these injection modes. But bulk shearing used in this paper seems to provide the most homogeneous distribution of energies inside the system at the onset of spreading.

F. Radjai would like to acknowledge the support of the ICoME2 Labex (ANR-11-LABX-0053) and the A*MIDEX projects (ANR-11-IDEX-0001-02) cofunded by the French program Investissements d'Avenir.

Author contribution statement

All authors contributed equally to this paper.

References

1. S.B. Savage, J. Fluid Mech. **92**, 53 (1979).
2. C. Campbell, Ann. Rev. Fluid Mech. **22**, 57 (1990).
3. GDR-MiDi, Eur. Phys. J. E **14**, 341 (2004).
4. D.L. Henann, K. Kamrin, Proc. Natl. Acad. Sci. U.S.A. **110**, 6730 (2013).
5. A. Daerr, S. Douady, Nature **399**, 241 (1999).
6. M. Pailha, M. Nicolas, O. Pouliquen, Phys. Fluids **20**, 111701 (2008).
7. M.J. Woodhouse, A.R. Thornton, C.G. Johnson, B.P. Kokelaar, J.M.N.T. Gray, J. Fluid Mech. **709**, 543 (2012).
8. O. Hungr, S.G. Evans, M.J. Bovis, J.N. Hutchinson, Environ. Engin. Geosci. **7**, 221 (2001).
9. D.G. Masson, C.B. Harbitz, R.B. Wynn, G. Pedersen, F. Lovholt, Philos. Trans. R. Soc. A **364**, 2009 (2006).
10. K. Hewitt, Am. Sci. **98**, 410 (2010).
11. D. Keeper, Geol. Soc. Am. Bull. **95**, 406 (1984).
12. M.A. Hampton, H.J. Lee, J. Locat, Rev. Geophys. **34**, 33 (1996).
13. K. Hutter, T. Koch, C. Pluss, S.B. Savage, Acta Mech. **109**, 127 (1995).
14. V. Buchholtz, T. Pschel, J. Stat. Phys. **84**, 1373 (1996).
15. R.M. Iverson, Rev. Geophys. **35**, 245 (1997).
16. F. Legros, Engin. Geol. **63**, 301 (2002).
17. G. Lube, H.E. Huppert, R.S.J. Sparks, M.A. Hallworth, J. Fluid Mech. **508**, 175 (2004).
18. E. Lajeunesse, A. Mangeney-Castelnau, J.P. Vilotte, Phys. Fluids **16**, 2371 (2004).
19. S. Siavoshi, A. Kudrolli, Phys. Rev. E **71**, 051302 (2005).
20. N.J. Balmforth, R.R. Kerswell, J. Fluid Mech. **538**, 399 (2005).
21. E. Lajeunesse, J.B. Monnier, G.M. Homsy, Phys. Fluids **17**, 103302 (2005).
22. L.E. Silbert, J.W. Landry, G.S. Grest, Phys. Fluids **15**, 1 (2003).
23. N. Jain, J.M. Ottino, R.M. Lueptow, J. Fluid Mech. **508**, 23 (2004).
24. R. Zenit, Phys. Fluids **17**, 031703 (2005).
25. L. Staron, E.J. Hinch, J. Fluid Mech. **545**, 1 (2005).
26. L. Staron, Geophys. J. Int. **172**, 455 (2008).
27. L. Staron, E. Lajeunesse, Geophys. Res. Lett. **36**, L12402 (2009).
28. V. Topin, Y. Monerie, F. Perales, F. Radjai, Phys. Rev. Lett. **109**, 188001 (2012).
29. P. Mutabaruka, J.-Y. Delenne, K. Soga, F. Radjai, Phys. Rev. E **89**, 052203 (2014).
30. F. Radjai, S. Roux, Phys. Rev. Lett. **89**, 064302 (2002).
31. J.J. Moreau, *New computation methods in granular dynamics*, in *Powders & Grains 93* (A. A. Balkema, Rotterdam, 1993) p. 227.
32. M. Jean, Comput. Methods Appl. Mech. Engin. **177**, 235 (1999).
33. F. Radjai, V. Richefeu, Mech. Mater. **41**, 715 (2009).
34. F. Radjai, F. Dubois (Editors), *Discrete-element Modeling of Granular Materials* (Iste-Wiley, London, 2011).
35. N. Estrada, A. Taboada, F. Radjaï, Phys. Rev. E **78**, 021301 (2008).